

Article

Optimal Synthesis of Five-Bar Linkage Based on Singularity-Free Workspaces with Predefined Shapes

Lovasz Erwin-Christian , Ciupe Valentin *, Demjen Tivadar, Oarcea Alexandru , Tulcan Elida-Gabriela  and Sandu Melania-Olivia

Department of Mechatronics, University Politehnica Timișoara, 300006 Timisoara, Romania; erwin.lovasz@upt.ro (L.E.-C.); tivadar.demjen@student.upt.ro (D.T.); alexandru.oarcea@student.upt.ro (O.A.); elida.tulcan@upt.ro (T.E.-G.); melania.sandu@upt.ro (S.M.-O.)

* Correspondence: valentin.ciupe@upt.ro

Abstract: The five-bar linkage, used in the form of a planar manipulator, benefits from easy controllability and relatively simple kinematic structures, which mean that it can be used in several applications in robotics, rehabilitation, and haptic devices, etc. This paper proposes an optimal synthesis method for a symmetrical five-bar linkage of type 5-RRRRR, with a singularity-free dexterous workspace, based on workspaces with predefined shapes, like squares, rectangles, triangles, circles, and ellipses. The synthesis conditions, to avoid singularities, are given as inequations, which can be further substituted with a system of equations, by introducing the supraunitary coefficient, k . The analytical solutions of the resulting system of equations enable the computation of the link lengths of the five-bar linkage. The optimization method provides the optimal value of the supraunitary coefficient, in order to obtain a maximum value for the minimum input transmission angle and a minimum value for the manipulator size. In this paper, the authors present an analytical approach to the optimal synthesis of a symmetrical five-bar linkage for different shapes of workspace, with the same surface and coordinates in terms of the mass center, as well as the resulting link lengths. In regard to the numerical examples, the authors considered and compared performance indices, such as manipulability, the condition number, and stiffness. The considered examples showed that an equilateral triangle-shaped workspace achieved higher global manipulability, a square-shaped workspace achieved higher global dexterity and the minimum input transmission angle, and circular workspaces achieved the highest mean stiffness and total surface size. It was observed that the synthesis method generates structures that are well-suited to singularity-free dexterous workspaces, with nonzero stiffness values.

Keywords: five-bar linkage; planar manipulator; optimal synthesis; singularity-free workspace; performance indices



Citation: Erwin-Christian, L.; Valentin, C.; Tivadar, D.; Alexandru, O.; Elida-Gabriela, T.; Melania-Olivia, S. Optimal Synthesis of Five-Bar Linkage Based on Singularity-Free Workspaces with Predefined Shapes. *Robotics* **2024**, *13*, 173. <https://doi.org/10.3390/robotics13120173>

Academic Editor: Raffaele Di Gregorio

Received: 30 October 2024

Revised: 24 November 2024

Accepted: 29 November 2024

Published: 5 December 2024



Copyright: © 2024 by the authors. Licensee MDPI, Basel, Switzerland. This article is an open access article distributed under the terms and conditions of the Creative Commons Attribution (CC BY) license (<https://creativecommons.org/licenses/by/4.0/>).

1. Introduction

Five-bar linkages are a type of planar parallel manipulator, with two connecting paths to the characteristic point used as complex path-generating mechanisms, involving the correlation and motion control of two servo actuators. Because of their easy controllability and relatively simple kinematic structures [1], planar manipulators are a core type of robotic system that are widely employed in precision manufacturing, industrial automation, and medical and agricultural devices. The literature describes several applications of five-bar linkages, namely as a double SCARA robot [2,3], as a parallel manipulator for high-speed and precision positioning of the end-effector using an over constrained structure [4], as haptic devices for wearable display LinkTouch [5], as a polycentric knee prosthesis joint [6], as robotic interfaces to facilitate neuro-rehabilitation [7], as a gait training and rehabilitation machine [8], as an automatized vegetable and potato planter [9,10], as an unmanned vegetable factory packing machine [11], and as a robot for pressurized

auto-sampling for enhanced oil recovery [12]. Many other research papers have studied different structures of five-bar linkages from the point of view of kinematic analysis [13–17], singularity analysis [18–20], analysis of the singularity-free workspace, dexterity [18–23], and control [24,25].

Ratolikar et al. in [26], carry out dimensional synthesis of a five-bar linkage for obtaining of the optimum workspace and with maximum dexterity, by using both a parametric study and the simplex algorithm. In [27], Nafees et al. proposed a form of dimensional synthesis, based on dyadic and triadic techniques, for different topologies of the planar five-bar linkage, which transmits motion between two extreme positions. The synthesis of a five-bar linkage as a function generator is analytically formulated with an objective function expressed in polynomial form, performed with equal spacing and using the Chebyshev approximation method, as described in [28] by Kiper et al. respectively regarding equal spacing and squares approximation in [29]. Sen et al. in [30], propose an optimal design of a five-bar planar manipulator to minimize the shaking force and shaking moments. Tivadar et al. in [31–33], propose an analytical method for the dimensional synthesis of a five-bar linkage based on the avoidance of singularities in a predefined workspace. The length of the links is the result of an equation system obtained from the conditions necessary to avoid singularities, given as inequations, by introducing the supraunitary coefficient, k . In [34], Tivadar proposed an optimization method with the aim of maximizing the minimum input transmission angle and the minimum manipulability.

The aim of this study is to develop a general analytical equation system for the synthesis of a five-bar linkage several workspaces with predefined shapes. For this purpose, an optimum synthesis method, based on minimizing the size of the surface of a five-bar linkage manipulator and on maximizing the minimum input transmission angle, will be proposed. The optimized design of a five-bar linkage for several workspace shapes, with the same surface size and coordinates in terms of the mass center, will be compared regarding the performance indices: manipulability, condition number, and stiffness.

2. General Analytical Synthesis Method for Symmetrical Five-Bar Linkages

The analytical synthesis method proposed in [31–34] considers the predefined dexterous workspace of a symmetrical five-bar linkage of type 5-RRRRR without singularities to have a square shape. The current general analytical synthesis method should be adequate for several shapes of predefined singularity-free workspaces, like squares, rectangles, triangles, circles, or ellipses.

The general conditions for avoiding singularities in a dexterous workspace, which relates to folded or extended positions of neighboring links (links 2 and 3, and links 3 and 4, respectively) are expressed in the following equations [31,32] (see Figure 1a,b):

$$|l_3 - l_2| < y_{Mmin}, \quad (1)$$

$$l_2 + l_3 > \sqrt{(x_{Mmax} + l_1/2)^2 + y_{Mmax}^2}, \quad (2)$$

$$l_1 \leq 2(l_3 - l_2), \quad (3)$$

where the coordinates of the points M_{min} (x_{Mmin}, y_{Mmin}) and M_{max} (x_{Mmax}, y_{Mmax}) relate to the closest and the farthest point of the workspace in regard to the frame joint A_0 .

Because of the symmetrical design of the five-bar linkage, the first two conditions are the same for the opposite chain, E_0DC (see Figure 1b). For an analytical solution to the general synthesis method, it is necessary to transform the previous inequations into an equation system, by considering a supraunitary coefficient $k > 1$ multiplied with the lower term in the inequation and accepting $l_3 > l_2$:

$$k \cdot (l_3 - l_2) = y_{Mmin} \quad (4)$$

$$l_2 + l_3 = k \cdot \sqrt{(x_{Mmax} + l_1/2)^2 + y_{Mmax}^2} \quad (5)$$

$$k \cdot l_1 = 2(l_3 - l_2) \quad (6)$$

The equation system allows the computation of the length of the links in the five-bar linkage in the form:

$$l_1(k) = 2y_{Mmin}/k^2 \quad (7)$$

$$l_2(k) = \frac{1}{2} \left(k \sqrt{(x_{Mmax} + l_1/2)^2 + y_{Mmax}^2} - \frac{1}{k} y_{Mmin} \right) \quad (8)$$

$$l_3(k) = \frac{1}{2} \left(k \sqrt{(x_{Mmax} + l_1/2)^2 + y_{Mmax}^2} + \frac{1}{k} y_{Mmin} \right) \quad (9)$$

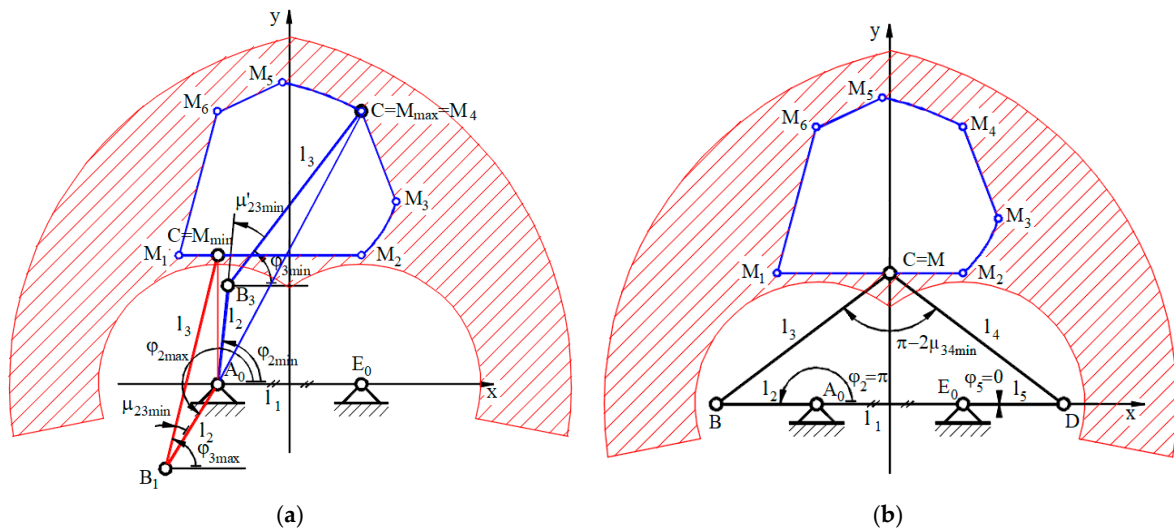


Figure 1. General analytical synthesis method for symmetrical five-bar linkages regarding a dexterous, singularity-free workspace: (a) conditions for the folded and extended positions of links 2 and 3; (b) conditions for the extended positions of links 3 and 4.

3. Optimization of the General Synthesis Method

The optimization of the general synthesis method computes the optimal value of the supraunitary coefficient, k_{opt} , by defining a target function to maximize the minimum input transmission angle, $\mu_{23min}(k)$, and minimizing the total size of the surface of the five-bar linkage, $S_t(k)$. That means, a higher value for the input transmission angle is required to allow for better transmission of the drive forces and to reduce the total size of the rectangle of the five-bar linkage.

The target function for the optimization method contains the normalized minimum input transmission angle, $\overline{\mu_{23min}}$, and the normalized total size of the surface of the rectangle of the five-bar linkage, $\overline{S_t}$, with the weight coefficients, p_1 and p_2 . The value of the coefficient k_{sol} results from the maximum value of the target function:

$$F(k) = p_1 \cdot \overline{\mu_{23min}}(k) - p_2 \cdot \overline{S_t}(k) \rightarrow \max, \quad (10)$$

where:

$$\overline{\mu_{23min}}(k) = \frac{\mu_{23min}(k) - \mu_{23min}(k)|_{min}}{\mu_{23min}(k)|_{max} - \mu_{23min}(k)|_{min}}, \quad (11)$$

$$\overline{S_t}(k) = \frac{S_t(k) - S_t(k)|_{min}}{S_t(k)|_{max} - S_t(k)|_{min}}, \quad (12)$$

with the minimum input transmission angle:

$$\mu_{23min}(k) = \arccos\left(\frac{l_2^2(k) + l_3^2(k) - y_{Mmin}^2}{2l_2(k) \cdot l_3(k)}\right), \quad (13)$$

the rectangular total size surface of the five-bar linkage:

$$S_t(k) = l_x(k) \cdot l_y(k), \quad (14)$$

and the lengths of the links in the synthesized five-bar linkage in the x and y direction are considered for the whole linkage and represent their maximum value:

$$l_x(k) = l_1(k) + 2 \cdot l_2(k), \quad l_y(k) = y_{Mmax} + l_2(k) \cdot \sin(\beta(k) - \frac{\pi}{2}), \quad (15)$$

where:

$$\beta(k) = \arccos\left(\frac{l_2^2(k) + y_{Mmin}^2 - l_3^2(k)}{2l_2(k) \cdot y_{Mmin}}\right). \quad (16)$$

4. Numerical Examples Using the Optimized General Synthesis Method

The optimized general synthesis method was applied regarding some numerical examples for several shapes of desired workspace. To further compare the performance of the synthesized five-bar linkage, the coordinates of the center of mass and the size of the surface of the desired workspace were considered as common parameters. The characteristic points, M_{min} and M_{max} , of the workspace shape are computed for each considered case. To provide values closer to the extreme values for both the normalized minimum input transmission angle μ_{23min} and the normalized total size of the surface of the rectangle of the five-bar linkage S_t , the weight parameters that are chosen are equal.

4.1. Five-Bar Linkage with Square-Shaped Singularity-Free Workspace

For the desired workspace with a square shape, it is necessary to compute the length of the side of the square, which is possible by using the well-known relationship in terms of a square surface and the coordinates of the characteristic points M in the workspace (see Table 1).

Table 1. Specific parameters of the square-shaped workspace.

Parameter	Denotation	Value
Side length of the square	l	200 mm
Minimum position of the characteristic point	$x_{Mmin} = l_1$	to be computed
	y_{Mmin}	130 mm
Maximum position of the characteristic point	x_{Mmax}	100 mm
	y_{Mmax}	330 mm

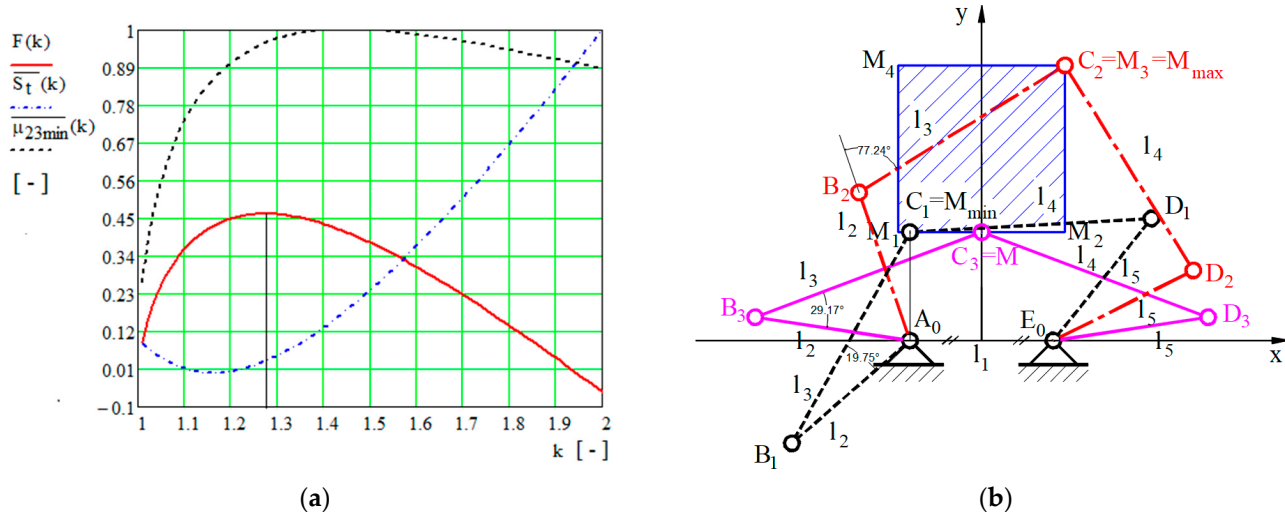
Figure 2a shows the variation in the normalized minimum input transmission angle μ_{23min} , the normalized rectangular total size of the surface of the five-bar linkage S_t , and the target function F in regard to the range of the coefficient $k \in (1.0, 2.0)$, and in regard to the input values presented in Tables 1 and 2. The maximum value of the normalized minimum input transmission angle occurs for the coefficient at $k = 1.46$, the minimum value of the total size of the surface of the five-bar linkage is $k = 1.15$, and the maximum value of the target function is $k = 1.27$. The geometrical parameters of the optimized five-bar linkage are detailed in Table 3 and are shown regarding the critical points in Figure 2b.

Table 2. Common parameters of the desired workspace.

Parameter	Denotation	Value
Coordinates of the center of mass	x_G	0 mm
	y_G	230 mm
Surface of the workspace	S_w	40.000 mm ²
Weight coefficients	p_1	0.5
	p_2	0.5

Table 3. Geometrical parameters of the optimized five-bar linkage.

Parameter	Denotation	Value
Length of link 1	l_1	161.2 mm
Length of links 2 and 5	$l_2 = l_5$	187.7 mm
Length of links 3 and 4	$l_3 = l_4$	290.1 mm
Minimum input transmission angle	μ_{23min}	19.77°
Total size of the surface of the five-bar linkage	S_t	243.100 mm ²

**Figure 2.** Optimized five-bar linkages with square-shaped dexterous singularity-free workspace: (a) variation in the normalized minimum transmission angle $\bar{\mu}_{23min}(k)$, the total size of the surface $\bar{S}_t(k)$, and the target function $F(k)$; (b) kinematic schema of the synthesized five-bar linkage in terms of the critical positions.

4.2. Five-Bar Linkage with Rectangular-Shaped Singularity-Free Workspace

For a workspace with a rectangular shape, the length of the rectangle is imposed and the width of the rectangle is computed by using the relationship in terms of the rectangle surface. Also, the coordinates of the characteristic points M in the workspace must be computed, accordingly (see Table 4).

Table 4. Specific parameters of the rectangular workspace.

Parameter	Denotation	Value
Length of the rectangle	L	250 mm
Width of the rectangle	l	160 mm
Minimum position of the characteristic point	$x_{Mmin} = l_1$	to be computed
	y_{Mmin}	105 mm
Maximum position of the characteristic point	x_{Mmax}	80 mm
	y_{Mmax}	355 mm

Figure 3a shows the variation in the normalized functions $\bar{\mu}_{23min}(k)$, $\bar{S}_t(k)$, and the target function $F(k)$ for coefficient $k \in (1.0, 2.0)$ and the values detailed in Tables 1 and 4. The maximum value of the normalized minimum input transmission angle occurs for the coefficient at $k = 1.43$, the minimum value of the total size of the surface of the five-bar linkage occurs at $k = 1.04$, and the maximum value of the target function occurs at $k = 1.23$. The geometrical parameters of the optimized five-bar linkage are detailed in Table 5 and the critical points are shown in Figure 4b.

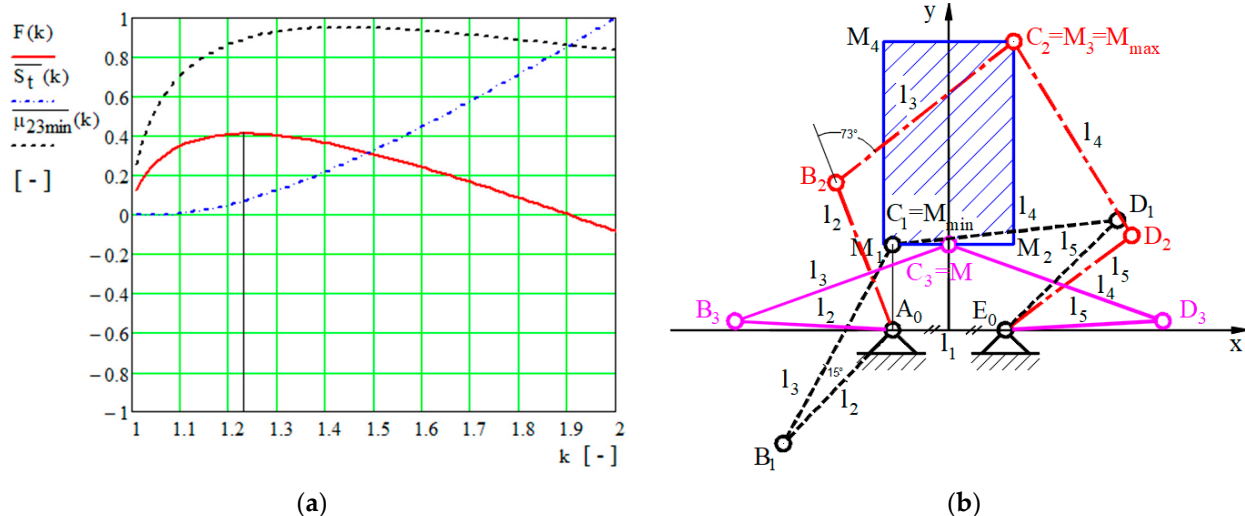


Figure 3. Optimized five-bar linkages with rectangular-shaped dexterous singularity-free workspace: (a) variation in the normalized minimum transmission angle $\bar{\mu}_{23min}(k)$, the total size of the surface $\bar{S}_t(k)$, and the target function $F(k)$; (b) kinematic schema of the synthesized five-bar linkage in terms of the critical positions.

Table 5. Geometrical parameters of the optimized five-bar linkage.

Parameter	Denotation	Value
Length of link 1	l_1	138.8 mm
Length of links 2 and 5	$l_2 = l_5$	194.2 mm
Length of links 3 and 4	$l_3 = l_4$	279.5 mm
Minimum input transmission angle	μ_{23min}	15.07°
Total size of the surface of the five-bar linkage	S_t	261.000 mm ²

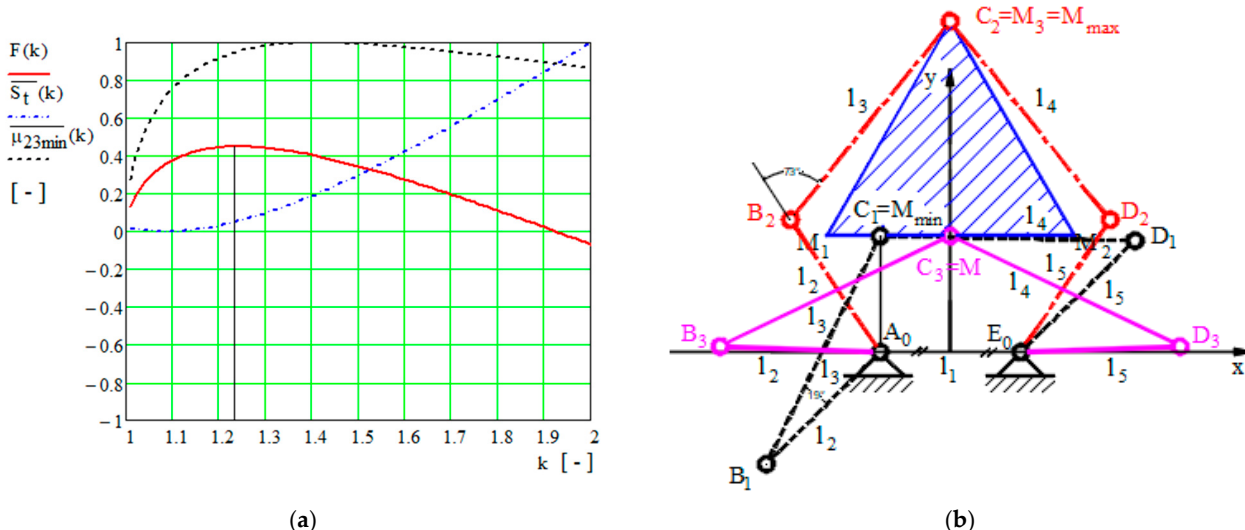


Figure 4. Optimized five-bar linkages with equilateral triangle-shaped dexterous singularity-free workspace: (a) variation in the normalized minimum transmission angle $\bar{\mu}_{23min}(k)$, the total size of the surface $\bar{S}_t(k)$, and the target function $F(k)$; (b) kinematic schema of the synthesized five-bar linkage in terms of the critical positions.

4.3. Five-Bar Linkage with Equilateral Triangle Shape Regarding the Desired Singularity-Free Workspace

For a workspace with an equilateral triangle shape, the length of the side is computed by using the well-known relationship in terms of the surface of an equilateral triangle.

Also, the coordinates of the characteristic points M in the workspace must be computed, accordingly (see Table 4).

Figure 4a shows the same variations in the normalized functions $\overline{\mu_{23min}}(k)$, $\overline{S_t}(k)$, and the target function $F(k)$ in the considered range for the coefficient k and for the values detailed in Tables 1 and 6. The maximum value of the normalized minimum input transmission angle occurs for the coefficient at $k = 1.41$, the minimum value of the total size surface of the five-bar linkage occurs at $k = 1.08$, and the maximum value of the target function occurs at $k = 1.22$. The specific parameters of the optimized five-bar linkage are detailed in Table 7 and the critical points are shown in Figure 4b.

Table 6. Specific parameters of the equilateral triangle-shaped workspace.

Parameter	Denotation	Value
Length of the side of the equilateral triangle	L	303.9 mm
Minimum position of the characteristic point	$x_{Mmin} = l_1$	to be computed
	y_{Mmin}	142.3 mm
Maximum position of the characteristic point	x_{Mmax}	0 mm
	y_{Mmax}	405.5 mm

Table 7. Geometrical parameters of the optimized five-bar linkage.

Parameter	Denotation	Value
Length of link 1	l_1	191.2 mm
Length of links 2 and 5	$l_2 = l_5$	195.8 mm
Length of links 3 and 4	$l_3 = l_4$	312.5 mm
Minimum input transmission angle	μ_{23min}	18.96°
Total size of the surface of the five-bar linkage	S_t	316.300 mm ²

4.4. Five-Bar Linkage with Circular-Shaped Singularity-Free Workspace

For a workspace with a circular shape, the radius length is computed by using the relationship in terms of the circle's surface. Because the minimum coordinate of the characteristic point M_{min} is on the y -axis, which is normal regarding a circle, the value of the frame length is set to zero ($l_1 = 0$), even though the relationship (7) gives a finite value. The coordinates of the characteristic points M in the workspace are detailed in Table 8.

Table 8. Specific parameters of the circular-shaped workspace.

Parameter	Denotation	Value
Radius of the circle	R	112.8 mm
Minimum position of the characteristic point	$x_{Mmin} = l_1$	0 mm
	y_{Mmin}	117.2 mm
Maximum position of the characteristic point	x_{Mmax}	0 mm
	y_{Mmax}	342.8 mm

The variations in the normalized functions $\overline{\mu_{23min}}(k)$, $\overline{S_t}(k)$, and the target function $F(k)$ in the range of $k \in (1.0, 2.0)$ for the values provided in Table 8 are shown in Figure 5a. The maximum value of the normalized minimum input transmission angle occurs for the coefficient at $k = 1.39$ and the minimum value of the total size of the surface of the five-bar linkage occurs at $k = 1.0$. As shown in Figure 5a, the total size of the surface increases linearly and the maximum value of the target function is reached at $k = 1.18$. The specific parameters of the optimized five-bar linkage are detailed in Table 9 and the critical points are shown in Figure 5b. It is also worth highlighting that the rotational joints A_0 and E_0 are superposed, an occurrence that reduced the total size of the surface of the five-bar linkage.

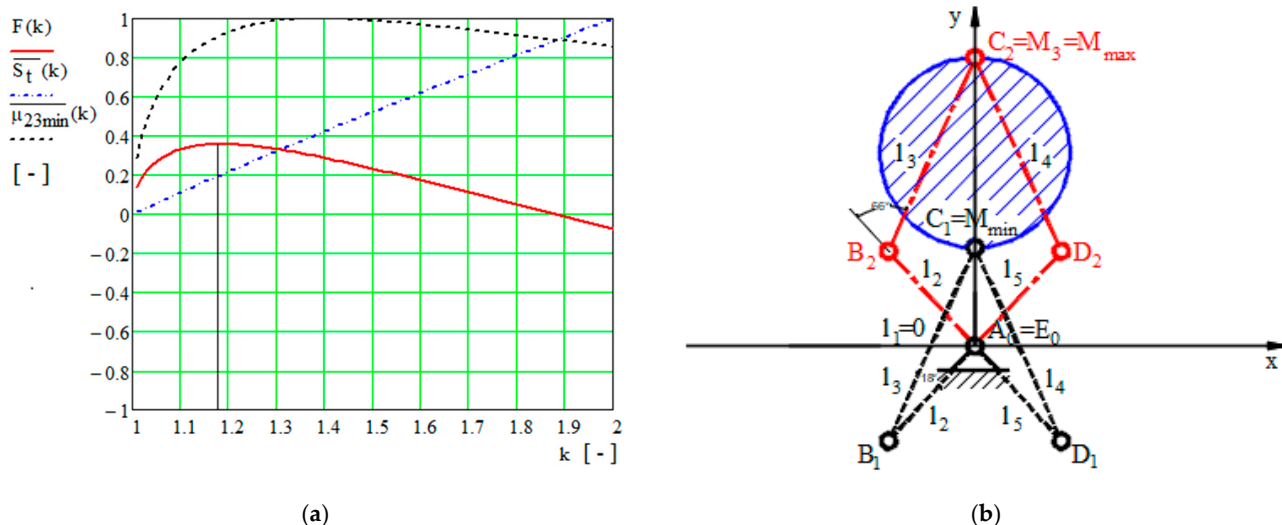


Figure 5. Optimized five-bar linkages with circular-shaped dexterous singularity-free workspace: (a) variation in the normalized minimum transmission angle $\bar{\mu}_{23min}(k)$, the total size of the surface $\bar{S}_t(k)$, and the target function $F(k)$; (b) kinematic schema of the synthesized five-bar linkage in terms of the critical positions.

Table 9. Geometrical parameters of the optimized five-bar linkage.

Parameter	Denotation	Value
Length of link 1	l_1	0 mm
Length of links 2 and 5	$l_2 = l_5$	152.6 mm
Length of links 3 and 4	$l_3 = l_4$	251.9 mm
Minimum input transmission angle	$\bar{\mu}_{23min}$	18.26°
Total size of the surface of the five-bar linkage	S_t	139.000 mm ²

4.5. Five-Bar Linkage with Elliptical-Shaped Singularity-Free Workspace

For a workspace with an elliptical shape, the length of the semi-major axis is imposed and the length of the semi-minor axis is computed by using the relationship in terms of the surface of the ellipse. Because the minimum coordinate of the characteristic point M_{min} is on the y -axis, the value of the frame length is set to zero ($l_1 = 0$). The calculated coordinates of the characteristic points M in the workspace are shown in Table 8.

The variations in the normalized functions $\bar{\mu}_{23min}(k)$, $\bar{S}_t(k)$, and the target function $F(k)$ in the range of $k \in (1.0, 2.0)$ for the values detailed in Table 10 are shown in Figure 6a. The maximum value of the normalized minimum input transmission angle occurs for the coefficient at $k = 1.40$ and the minimum value of the total size of the surface of the five-bar linkage occurs at $k = 1.0$. As shown in Figure 6a, the total size of the surface increases linearly and the maximum value of the target function is reached at $k = 1.16$. The specific parameters of the optimized five-bar linkage are detailed in Table 11 and the critical points are shown in Figure 6b. The rotational joints A_0 and E_0 are superposed, which means that total size of the surface of the five-bar linkage is reduced.

Table 10. Specific parameters of the elliptical-shaped workspace.

Parameter	Denotation	Value
Length of the semi-major axis	a	130 mm
Length of the semi-minor axis	b	97.9 mm
Minimum position of the characteristic point	$x_{Mmin} = l_1$	0 mm
	y_{Mmin}	100 mm
Maximum position of the characteristic point	x_{Mmax}	0 mm
	y_{Mmax}	360 mm

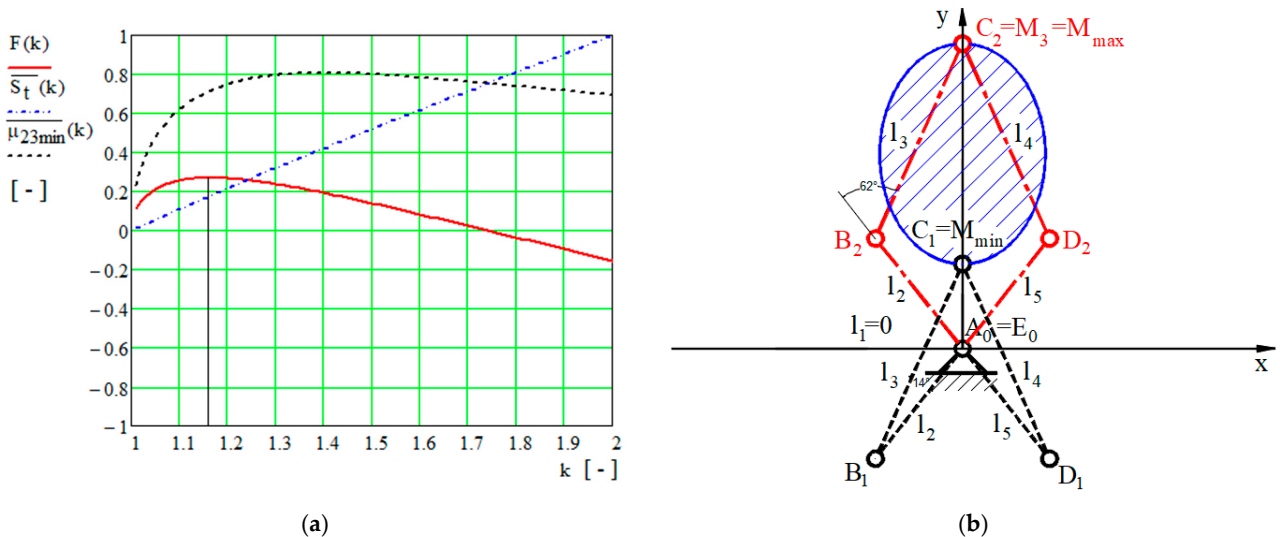


Figure 6. Optimized five-bar linkages with elliptical-shaped dexterous singularity-free workspace: (a) variation in the normalized minimum transmission angle $\bar{\mu}_{23min}(k)$, the total size of the surface $\bar{S}_t(k)$, and the target function $F(k)$; (b) kinematic schema of the synthesized five-bar linkage in terms of the critical positions.

Table 11. Geometrical parameters of the optimized five-bar linkage.

Parameter	Denotation	Value
Length of link 1	l_1	0 mm
Length of links 2 and 5	$l_2 = l_5$	165.7 mm
Length of links 3 and 4	$l_3 = l_4$	251.9 mm
Minimum input transmission angle	$\bar{\mu}_{23min}$	14.25°
The total size of the surface of the five-bar linkage	S_t	162.400 mm ²

5. Performance Analysis of the Optimized Five-Bar Linkage

The computation of the performance analysis involves the determination of the Jacobian matrix. The Jacobian matrix is computed as follows [35–37]:

$$J = J_x^{-1} \cdot J_q \quad (17)$$

where J_q and J_x are:

$$J_q = \begin{bmatrix} \frac{\partial F_2(X, Q)}{\partial \varphi_2} & \frac{\partial F_2(X, Q)}{\partial \varphi_5} \\ \frac{\partial F_5(X, Q)}{\partial \varphi_2} & \frac{\partial F_5(X, Q)}{\partial \varphi_5} \end{bmatrix}, \quad (18)$$

$$J_x = \begin{bmatrix} \frac{\partial F_2(X, Q)}{\partial x_M} & \frac{\partial F_2(X, Q)}{\partial y_M} \\ \frac{\partial F_5(X, Q)}{\partial x_M} & \frac{\partial F_5(X, Q)}{\partial y_M} \end{bmatrix}. \quad (19)$$

where the transmission functions are:

$$F_2(x_M, y_M) = A_2(x_M, y_M) \cos \varphi_2 + B_2(x_M, y_M) \sin \varphi_2 + C_2(x_M, y_M), \quad (20)$$

$$F_5(x_M, y_M) = A_5(x_M, y_M) \cos \varphi_5 + B_5(x_M, y_M) \sin \varphi_5 + C_5(x_M, y_M) \quad (21)$$

with:

$$A_2(x_M, y_M) = -l_2(2x_M + l_1), \quad B_2(x_M, y_M) = -2l_2y_M, \quad C_2(x_M, y_M) = x_M^2 + y_M^2 + \frac{l_1^2}{4} + l_2^2 - l_3^2 + l_1x_M \quad (22)$$

$$A_5(x_M, y_M) = -l_5(2x_M - l_1), \quad B_5(x_M, y_M) = -2l_5y_M, \quad C_5(x_M, y_M) = x_M^2 + y_M^2 + \frac{l_1^2}{4} + l_5^2 - l_4^2 - l_1x_M \quad (23)$$

The vector of the input parameters of the five-bar linkage is $Q = [\varphi_2 \varphi_5]^T$ and the vector of the output parameters is $X = [x_M y_M]^T$ (see Figure 7).

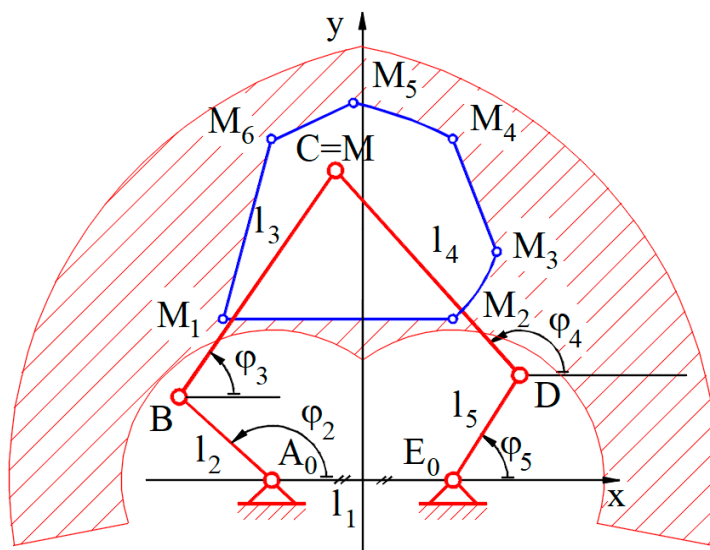


Figure 7. Kinematic schema of the symmetrical five-bar linkage.

In the following paragraphs the corresponding manipulability indices, condition number indices, and stiffness indices for the synthesized five-bar linkage are provided.

5.1. Manipulability Index for the Optimized Five-Bar Linkage with Different Workspace Shapes

The manipulability index (μ) characterizes the structures' ability to perform movements in any available direction in terms of the workspace, which was first introduced by Yoshikawa, and is computed as follows [38]:

$$\mu = |\det(J)| \quad (24)$$

The distributions in terms of the manipulability index were achieved for the previously presented numerical examples. Figure 8 shows the results for the minimal, maximal, and global values for all the shapes used in the synthesis examples in terms of the singularity-free workspaces.

Based on the results in Table 12 and the distributions in Figure 8, it can be observed that all the shapes for the inscribed workspaces are conducive to achieving link lengths according to which the resulting workspaces are singularity free. The triangular-shaped workspace appears to be the workspace with the highest achievable maneuverability and the highest global manipulability.

Table 12. Minimal, maximal, and mean values for the manipulability distributions.

Shape of the Workspace	Minimal Value [-]	Maximal Value [-]	Mean Value [-]
Square	$0.9777 \cdot 10^4$	$3.5291 \cdot 10^4$	$2.6303 \cdot 10^4$
Rectangle	$0.7343 \cdot 10^4$	$3.7795 \cdot 10^4$	$2.8247 \cdot 10^4$
Triangle	$1.2232 \cdot 10^4$	$5.3756 \cdot 10^4$	$3.2959 \cdot 10^4$
Circle	$1.05478 \cdot 10^4$	$3.3895 \cdot 10^4$	$2.6708 \cdot 10^4$
Ellipse	$0.9300 \cdot 10^4$	$3.5667 \cdot 10^4$	$2.8201 \cdot 10^4$

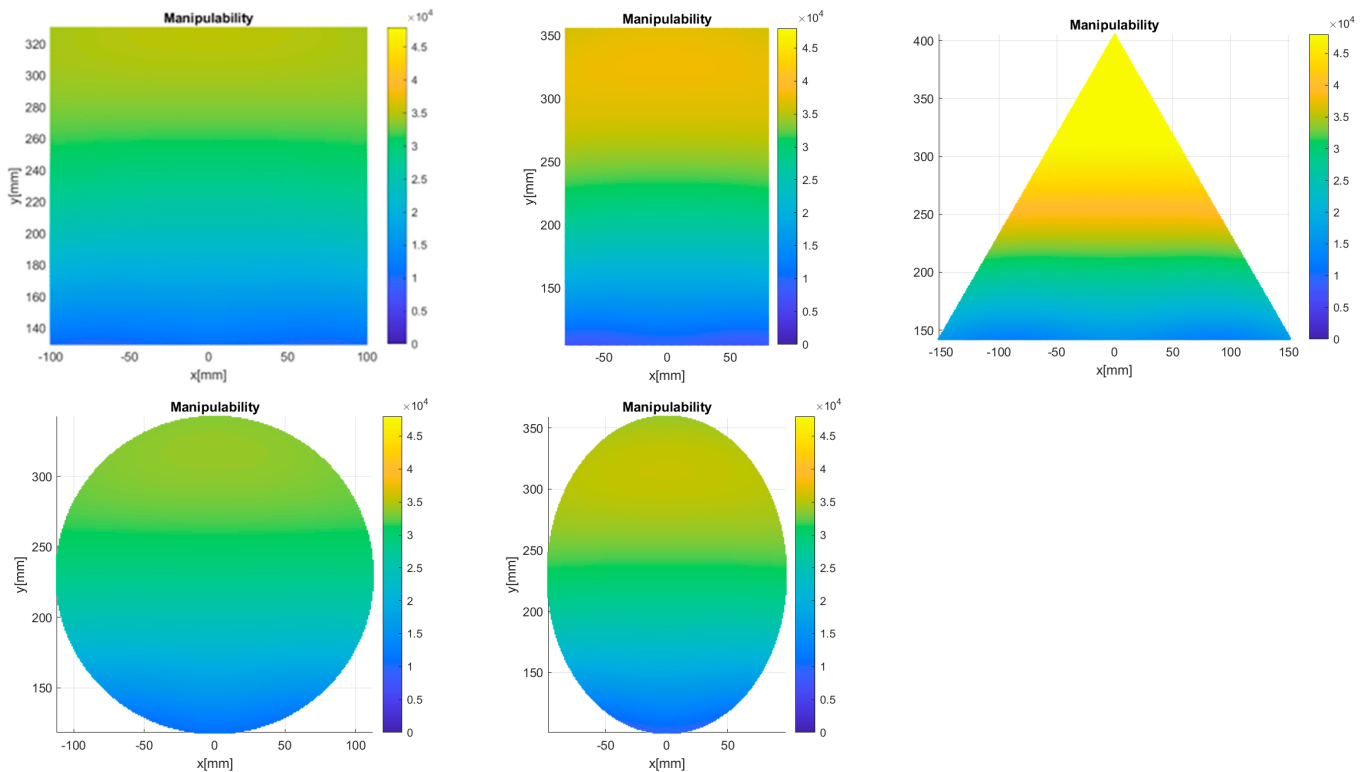


Figure 8. Manipability distributions inside the workspaces (square-shaped workspace (**top-left**), rectangular-shaped workspace (**top-center**), triangular-shaped workspace (**top-right**), circular-shaped workspace (**bottom-left**), and elliptical-shaped workspace (**bottom-right**)).

5.2. Condition Number Index for the Optimized Five-Bar Linkage with Different Workspace Shapes

The condition number index (K) is closely tied to the structure's dexterity. The computation of the condition number index is described as the ratio between the maximal and minimal values of the singular values (λ) in the Jacobian matrix [39,40].

$$K = \sqrt{\lambda_{max} / \lambda_{min}} \quad (25)$$

The distributions for the condition number index were achieved for the previously presented numerical examples. Figure 9 shows the results for the minimal, maximal, and global values for all the shapes used in the synthesis examples in regard to the dexterous workspaces.

Based on the results in Table 13 and the distributions in Figure 9, it can be observed that all the shapes for the workspaces are conducive to achieving link lengths according to which the resulting workspaces are dexterous. The elliptical-shaped workspace appears to be the workspace with the lowest achievable values for the condition number index, but the circular-shaped workspace appears to be the workspace with the lowest maximal values in terms of the condition number, while the square-shaped workspace is the most dexterous one, since the mean value of the condition number is the smallest.

Table 13. Minimal, maximal, and mean values for the condition number distributions.

Shape of the Workspace	Minimal Value [-]	Maximal Value [-]	Mean Value [-]
Square	1.0095	2.6115	1.6678
Rectangle	1.0022	3.0811	1.7548
Triangle	1.0740	2.9969	2.0573
Circle	1.0015	2.8134	1.7201
Ellipse	1.0007	3.1717	1.7694

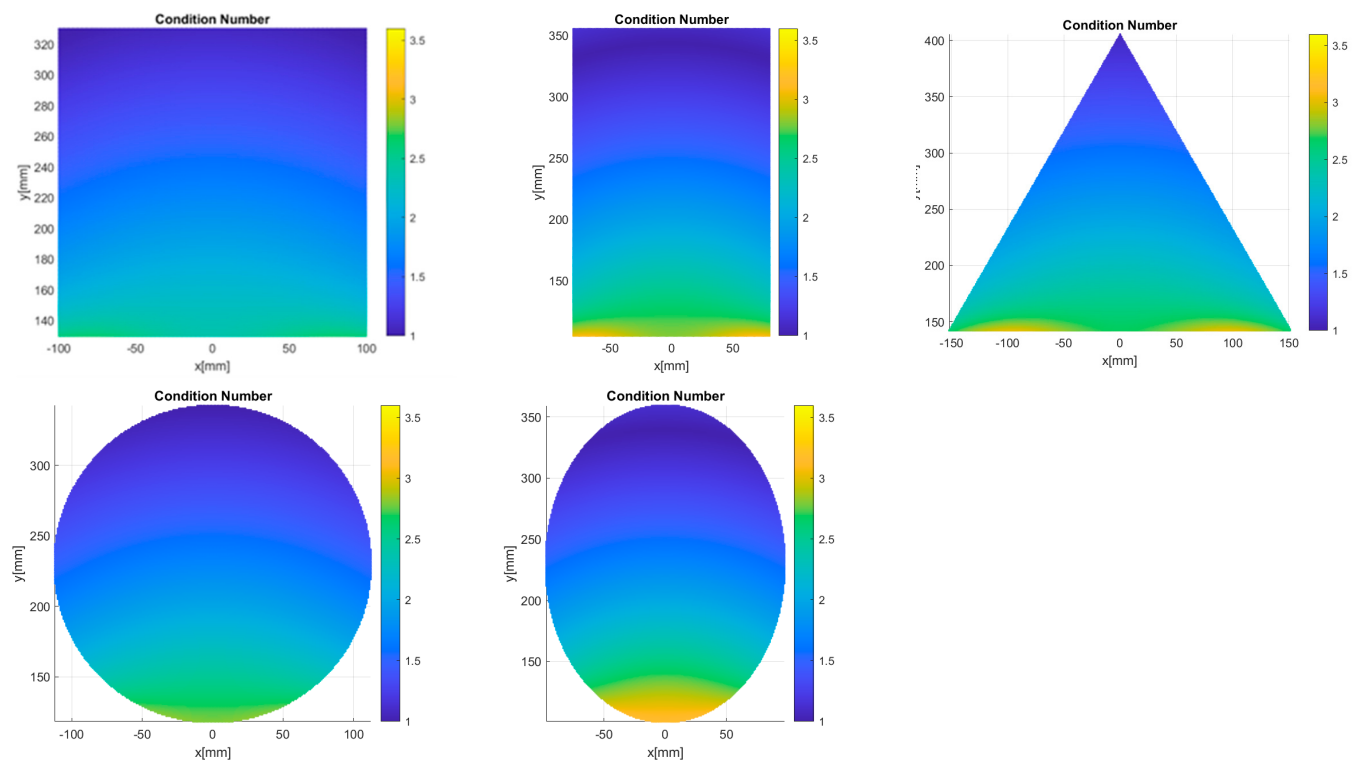


Figure 9. Condition number distributions inside the workspaces (square-shaped workspace (**top-left**), rectangular-shaped workspace (**top-center**), triangular-shaped workspace (**top-right**), circular-shaped workspace (**bottom-left**), elliptical-shaped workspace (**bottom-right**)).

5.3. Local Stiffness Index for the Optimized Five-Bar Linkage with Different Workspace Shapes

The local stiffness index (LSI) is computed in the same manner as the condition number index, but it is described as the ratio between the maximal and minimal values of the singular values of the product between the transposed Jacobian matrix and Jacobian matrix [39]. The distributions for the local stiffness index were achieved for the previously presented numerical examples. Table 14 shows the minimal, maximal, and global values for all the shapes used in the synthesis examples in terms of the workspaces, with stiffness values greater than zero.

Table 14. Minimal, maximal, and mean values for the local stiffness index distributions.

Shape of the Workspace	Minimal Value [-]	Maximal Value [-]	Mean Value [-]
Square	0.1466	0.9812	0.4295
Rectangle	0.1053	0.9956	0.4434
Triangle	0.1113	0.9753	0.4186
Circle	0.0956	0.9971	0.4552
Ellipse	0.0749	0.9997	0.4346

Based on the results in Table 13 and the distributions in Figure 10, it can be observed that all the shapes for the inscribed workspaces are conducive to achieving link lengths according to which the resulting workspaces lack positions in which the manipulator has no stiffness. The elliptical-shaped workspace appears to be the workspace with both the lowest and the highest achievable values for the local stiffness index, but the circular-shaped workspace appears to be the workspace with the highest value for the global stiffness index, thus being the most desirable one.

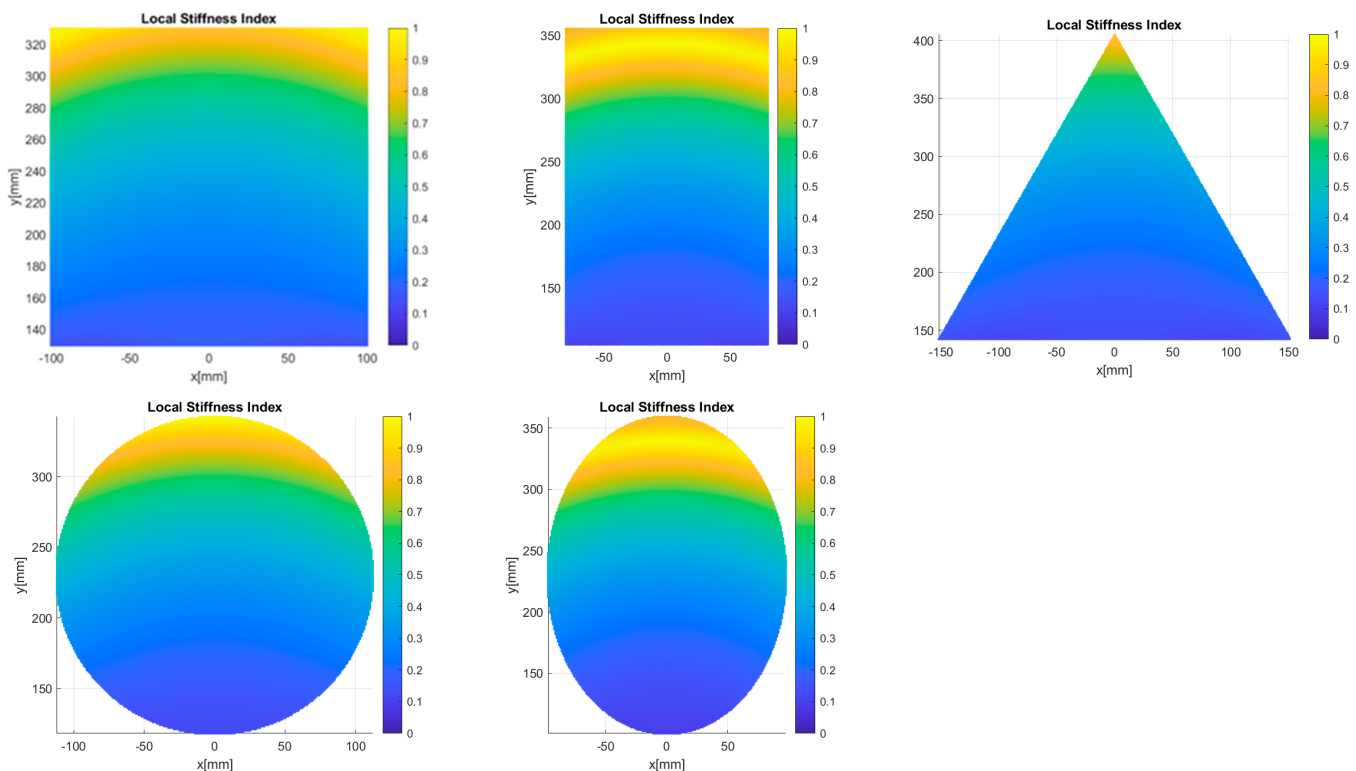


Figure 10. Local stiffness index distributions inside the workspaces (square-shaped workspace (**top-left**), rectangular-shaped workspace (**top-center**), triangular-shaped workspace (**top-right**), circular-shaped workspace (**bottom-left**), elliptical-shaped workspace (**bottom-right**)).

6. Conclusions

In this study, a novel analytical synthesis method for the five-bar linkage was presented. The novelty of the paper consists in developing an optimal general synthesis method for five-bar linkages with singularity-free dexterous workspaces. The method allows for the computation of the optimal values of the link lengths based on different shaped workspaces. The workspace shapes imposed in this paper are squares, rectangles, triangles, circles, and ellipses.

Based on the achieved results, it can be concluded that the generalized synthesis method was successful in determining the optimal link lengths of the five-bar linkage, based on the minimal size of the surface of the manipulator and the maximal minimum transmission angle.

Furthermore, all the analyzed workspaces are conducive of determining sets of optimal link lengths, such that the five-bar linkage resulting from the synthesis has a singularity-free and dexterous workspace, with nonzero stiffness values. The highest value of the minimum transmission angle is achieved for the singularity-free workspace with a square shape and the minimum total size of the surface belongs to the singularity-free workspace with a circular shape. It was observed that some shapes fit better than others when it comes to achieving higher performance metrics, such as the equilateral triangle-shaped workspace for achieving five-bar linkages with higher global manipulability, the square-shaped workspace for achieving five-bar linkages with higher global dexterity, and circular workspaces for achieving the highest mean stiffness.

Further research is proposed to investigate and observe the results of applying the synthesis method to linkages, serial structures with a higher degree of freedom, and parallel structures with a higher degree of freedom. Also, further research is proposed to investigate the effects on the k term, used in computing the link lengths, if maximal or minimal performance indices are used as scope functions, in addition to maximizing the minimum transmission angle and minimizing the workspace boundary of the synthesized structure.

Another further avenue of research, stimulated during the review process, should be the investigation of the influence of the weight coefficients of the target function and the ratio of the lengths of rectangular and elliptical workspaces on the geometrical and performance parameters of five-bar linkages.

Author Contributions: Conceptualization, L.E.-C. and D.T.; methodology, L.E.-C., C.V., D.T. and O.A.; software, O.A. and C.V.; validation, L.E.-C. and T.E.-G.; formal analysis, L.E.-C. and C.V.; investigation, D.T. and S.M.-O.; resources, O.A.; data curation, D.T., C.V. and S.M.-O.; writing—original draft preparation, L.E.-C., O.A. and T.E.-G.; writing—review and editing, L.E.-C., D.T., O.A. and T.E.-G.; visualization, O.A. and S.M.-O.; supervision, L.E.-C. and C.V. All authors have read and agreed to the published version of the manuscript.

Funding: This research received no external funding.

Data Availability Statement: No new data were created or analyzed in this study. Data sharing is not applicable to this article.

Acknowledgments: Special thanks go to Marco Ceccarelli for their support of this research.

Conflicts of Interest: The authors declare that there are no conflicts of interest.

References

1. Angeles, J. *Fundamentals of Robotic Mechanical Systems: Theory, Methods, and Algorithms*; Springer: Cham, Switzerland, 2014.
2. Tempea, I.; Neacșa, M.; Livadariu, A. A new acting solution of a double SCARA robot. In Proceedings of the 3rd International Conference on “Computational Mechanics and Virtual Engineering” COMEC 2009, Brasov, Romania, 29–30 October 2009; pp. 765–770.
3. Campos, L.; Bourbonnais, F.; Bonev, I.A.; Bigras, P. Development of a five-bar parallel robot with large workspace. In Proceedings of the ASME 2010 International Design Engineering Technical Conferences & Computers and Information in Engineering Conference IDETC/CIE 2010, Montreal, QC, Canada, 15–18 August 2010; pp. 917–922.
4. Kiper, G.; Dede, M.İ.C.; Uzunoğlu, E.; Mastar, E. Use of Hidden Robot Concept for Calibration of an Over-Constrained Mechanism. In Proceedings of the 14th IFTOMM World Congress, Taipei, Taiwan, 25–30 October 2015; Volume 4, pp. 243–247.
5. Tsetserukou, D.; Hosokawa, S.; Terashima, K. LinkTouch: A Wearable Haptic Device with Five-Bar Linkage Mechanism for Presentation of Two-DOF Force Feedback at the Fingerpad. In Proceedings of the IEEE Haptics Symposium, Houston, TX, USA, 23–26 February 2014; pp. 307–312.
6. Marzouk, W.W.; Ahmed, A.R. Analytical Model for Novel Design of Five-Bar Polycentric Knee Joint. In Proceedings of the International Conference on Pure and Applied Sciences (ICPAS 2015), Luxor, Egypt, 28–30 March 2015; pp. 1–13.
7. Klein, J.; Roach, N.; Burdet, E. 3DOM: A 3 Degree of Freedom Manipulandum to Investigate Redundant Motor Control. *IEEE Trans. Haptics* **2014**, *7*, 229–239. [[CrossRef](#)] [[PubMed](#)]
8. Seo, J.-W.; Kim, H.-S. Biomechanical Analysis in Five Bar Linkage Prototype Machine of Gait Training and Rehabilitation by IMU Sensor and Electromyography. *Sensors* **2021**, *21*, 1726. [[CrossRef](#)] [[PubMed](#)]
9. Sun, K.; Ge, R.; Li, T.; Wang, J. Design and Analysis of Vegetable Transplanter Based on Five-bar Mechanism. *IOP Conf. Ser. Mater. Sci. Eng.* **2019**, *692*, 012029. [[CrossRef](#)]
10. Sun, W.; Zhang, H.; Simionescu, P.A. Numerical optimization and experimental validation of a five-link mechanism, potato planter. *Proc. Inst. Mech. Eng. Part C J. Mech. Eng. Sci.* **2021**, *235*, 6883–6892. [[CrossRef](#)]
11. Zhang, L.; Liu, Y.; Chen, J.; Zhou, H.; Jiang, Y.; Tong, J.; Wu, L. Trajectory Synthesis and Optimization Design of an Unmanned Five-Bar Vegetable Factory Packing Machine Based on NSGA-II and Grey Relation Analysis. *Agriculture* **2023**, *13*, 1366. [[CrossRef](#)]
12. Jian, S. The Research of Five-Bar Robot for Pressurized Autosampling for Enhanced Oil Recovery Research. Master’s Thesis, Memorial University of Newfoundland, St. John’s, NFL, Canada, 26 October 2016.
13. Alici, G. An inverse position analysis of five-bar planar parallel manipulators. *Robotica* **2002**, *20*, 195–201. [[CrossRef](#)]
14. Joubair, A.; Slamani, M.; Bonev, I.A. Kinematic calibration of a five-bar planar parallel robot using all working modes. *Robot. Comput.-Integr. Manuf.* **2013**, *29*, 15–25. [[CrossRef](#)]
15. Simionescu, P.A.; Talpasanu, I. Kinematics of the eccentric RPRPR chain with applications to robotics, materials handling and manipulation. *Int. J. Mech. Robot. Syst.* **2014**, *2*, 314–340. [[CrossRef](#)]
16. Jiménez López, E.; Servín de la Mora-Pulido, D.; Servín de la Mora-Pulido, R.; Javier Ochoa-Estrella, F.; Acosta Flores, M.; Luna-Sandoval, G. Modeling in Two Configurations of a 5R 2-DoF Planar Parallel Mechanism and Solution to the Inverse Kinematic Modeling Using Artificial Neural Network. *IEEE Access* **2021**, *9*, 68583–68594. [[CrossRef](#)]
17. Shengqi, J.; Cheng, Y.; Luc, R.; Lesley, J. Five Bar Planar Manipulator Simulation and Analysis by Bond Graph. In Proceedings of the ASME 2014 International Mechanical Engineering Congress and Exposition, Montreal, QC, Canada, 14–20 November 2014. IMECE2014–37116.

18. Liu, X.-J.; Wanga, J.; Pritschow, G. Kinematics, singularity, and workspace of planar 5R symmetrical parallel mechanisms. *Mech. Mach. Theory* **2006**, *41*, 145–169. [[CrossRef](#)]
19. Theingi; Li, C.; Chen, I.-M.; Angeles, J. Singularity management of 2DOF planar manipulator using coupled kinematics. In Proceedings of the 7th International Conference on Control, Automation, Robotics and Vision (ICARCV'02), Singapore, 2–5 December 2002; pp. 402–407.
20. Wang, J.; Nie, L.; Zhao, D.; Ren, J.; Wang, Q.; Sun, J. Equivalent Five-bar Linkages for the Singularity Analysis of Two-DOF Seven-bar Linkages. In Proceedings of the ASME 2017 International Design Engineering Technical Conferences and Computers and Information in Engineering Conference, Cleveland, OH, USA, 6–9 August 2017. DETC2017-67527.
21. Yao, W.; Dai, J.S. Workspace and Orientation Analysis of a Parallel Structure for Robotic Fingers. *J. Adv. Mech. Des. Syst. Manuf.* **2011**, *5*, 54–69. [[CrossRef](#)]
22. Huang, M. Design of a Planar Parallel Robot for Optimal Workspace and Dexterity. *Int. J. Adv. Robot. Syst.* **2011**, *8*, 176–183. [[CrossRef](#)]
23. Liu, X.-J.; Wanga, J.; Pritschow, G. Performance atlases and optimum design of the planar 5R symmetrical parallel mechanisms. *Mech. Mach. Theory* **2006**, *41*, 119–144. [[CrossRef](#)]
24. Roskam, R.; Luc, R. Five Bar Parallel Plotter based on Construction Kits and Open Source Development Environment. In Proceedings of the 9th International Conference on Control, Mechatronics and Automation (ICCMA), Luxembourg, 11–14 November 2021; pp. 182–187.
25. Can, F.C.; Şen, H. Real time controlled two dof five bar robot manipulator. In Proceedings of the International Symposium of Mechanism and Machine Science, AzC IFToMM—Azerbaijan Technical University, Baku, Azerbaijan, 11–14 September 2017; pp. 50–56.
26. Ratolikar, M.D.; Kumar, P.R. Optimized design of 5R planar parallel mechanism aimed at gait-cycle of quadruped robots. *J. Vibroeng.* **2022**, *24*, 104–115. [[CrossRef](#)]
27. Nafees, K.; Mohammad, A. Dimensional synthesis of a planar five-bar mechanism for motion between two extreme positions. *Aust. J. Mech. Eng. Aust.* **2017**, *16*, 74–81. [[CrossRef](#)]
28. Kiper, G.; Bilgincan, T.; Can, M.İ.C. Function generation synthesis of planar 5R mechanism. *Probl. Mech.* **2013**, *51*, 28–31.
29. Kiper, G.; Bağdadioğlu, B.; Bilgincan, T. Function synthesis of the planar 5R mechanism using least squares approximation. In *Advances in Robot Kinematics*; Lenarcic, J., Khatib, O., Eds.; Springer: Cham, Switzerland, 2014; pp. 69–76.
30. Sen, D.K.; Yıldız, A.; Kopmaz, O. Optimal Design of a Five-Bar Planar Manipulator and Its Controller by Using Different Algorithms for Minimum Shaking Forces and Moments for the Largest Trajectory in a Usable Workspace. *Machines* **2022**, *10*, 971. [[CrossRef](#)]
31. Tivadar, D.; Lovasz, E.-C.; Ceccarelli, M.; Sticlaru, C.; Lupuți, A.-M.-F. Analytical Synthesis of Five-Bar Linkage used for 3D Printer Structure. In Proceedings of the 4th International Conference of the IFToMM, Naples, Italy, 14–16 September 2022; Series: Mechanisms and Machine Science; Springer International Publishing: Cham, Switzerland, 2022; Volume 122, pp. 105–113.
32. Tivadar, D.; Lovasz, E.-C.; Ceccarelli, M.; Sticlaru, C.; Luputi, A.-M.-F.; Oarcea, A.; Silaghi-Perju, D.-C. Design of the five-bar linkage with singularity-free Workspace. *Robotica* **2023**, *41*, 3361–3379.
33. Tivadar, D.; Lovasz, E.-C.; Ceccarelli, M.; Russo, M.; Tulcan, E.-G.; Oarcea, A. Design of a 3D Printer with Five-Bar Linkage. In Proceedings of the 25th International Conference on System Theory, Control and Computing, Iasi, Romania, 20–23 October 2021; Series: Mechanisms and Machine Science; Springer International Publishing: Cham, Switzerland, 2024; Volume 154, pp. 51–59.
34. Tivadar, D.; Oarcea, A.; Tulcan, E.-G.; Lovasz, E.-C.; Silaghi-Perju, D.-C. Optimal Synthesis of the Five-Bar Linkages with symmetrical Structure by using imposed Trajectories for Home Training. *Environ. Eng. Manag. J.* **2023**; submitted.
35. Buium, F.; Duca, C.; Leonchi, D. Problems regarding singularities analysis of a 0/3/3 parallel mechanism. *Appl. Mech. Mater.* **2014**, *658*, 569–574. [[CrossRef](#)]
36. Buium, F.; Leonchi, D.; Doroftei, I. A Workspace Characterization of the 0/3/3R Parallel Mechanism. *Appl. Mech. Mater.* **2014**, *658*, 563–568. [[CrossRef](#)]
37. Buium, F.; Duca, C.; Doroftei, I.; Leonchi, D. Graphical shapes of the 2nd type singularities of a 3-RRR planar mechanism. *IOP Conf. Ser. Mater. Sci. Eng.* **2016**, *147*, 012085. [[CrossRef](#)]
38. Yoshikawa, T. Manipulability of robotic mechanisms. *Int. J. Robot. Res.* **1985**, *4*, 3–9. [[CrossRef](#)]
39. Patel, S.; Sobh, T. Manipulator Performance Measures—A Comprehensive Literature Survey. *J. Intell. Robot. Syst.* **2015**, *77*, 547–570. [[CrossRef](#)]
40. Gosselin, C.; Angeles, J. A global performance index for the kinematic optimization of robotic manipulators. *J. Mech. Des.* **1991**, *113*, 220–226. [[CrossRef](#)]

Disclaimer/Publisher’s Note: The statements, opinions and data contained in all publications are solely those of the individual author(s) and contributor(s) and not of MDPI and/or the editor(s). MDPI and/or the editor(s) disclaim responsibility for any injury to people or property resulting from any ideas, methods, instructions or products referred to in the content.